Dalton Transactions

ROYAL SOCIETY OF CHEMISTRY

PAPER

View Article Online
View Journal | View Issue

Cite this: *Dalton Trans.*, 2024, **53**, 10890

Synthesis, characterisation and antimicrobial activity of supramolecular cobalt-peptide conjugates†

Liudmila Janzen, Reece G. Miller and Nils Metzler-Nolte *

Herein, we describe the synthesis and characterisation of four new supramolecular cobalt conjugates of antimicrobial peptides functionalised with terpyridine ligands (L). Peptides were chosen based on the well-established arginine-tryptophan $(RW)_3$ motif, with terpyridine-derivatized lysine (Lys(tpy)) added to the sequence, or replacing tryptophan residues. Self-assembly of the antimicrobial peptides with Co $(BF_4)_2{\cdot}6H_2O$ formed exclusively CoL_2 dimers (for peptides with one tpy ligand each) and Co_2L_4 metallo-macrocycles (for peptides with two tpy ligands for each peptide), which could be 'locked' by oxidation of Co(+II) to Co(+III) with ammonium ceric nitrate. The Co-peptide complexes were characterised by mass spectrometry and in solution by NMR spectroscopy, including 2D diffusion ordered NMR spectroscopy (DOSY) which confirmed the proposed stoichiometries. The antimicrobial activity of the novel peptides and their metallo-supramolecular assemblies was investigated by determination of their minimal inhibitory concentration (MIC) against a panel of Gram-positive and Gram-negative bacteria. Complexation with cobalt increases the activity of the peptides in almost every case. Most of the new metal–peptide conjugates showed good activity against Gram-positive bacteria, including a multi-resistant *S. aureus* strain and the opportunistic pathogenic yeast *C. albicans* (down to 7 μmol l^{-1} for the most active Co_2L_4 derivate), a value that is increased five-fold compared to the lysine-derivatized peptide ligand alone. Interestingly, conjugates of the CoL_2 type also showed decent activity against Gram-negative bacteria including the WHO-flagged problematic *A. baumannii* strain (down to 18 μmol l^{-1} for the most active derivative).

Received 27th March 2024,
Accepted 23rd May 2024

DOI: 10.1039/d4dt00907j

rsc.li/dalton

Introduction

Metal ions play a key role in numerous biological processes. Due to their interaction with macromolecules such as enzymes, pro-hormones, membranes and presecretory granules, a variety of biological functions including catalytic, structural, and regulatory activities are realized. Certain metals may also exhibit toxicity towards bacteria and yeast, which has led to their application as antimicrobial agents since ancient times.[1] More recently, mechanistic studies have helped elucidate the toxic effects of metals on microbial cells, leading to an increased interest in the application of metal-based complexes as antimicrobial agents.[2–9] It has been demonstrated that certain metals damage antibiotic resistance biofilms,[10] inhibit metabolic pathways in a selective manner,[11] and can kill multidrug-resistant bacteria.[12] Beyond small molecular compounds, large self-assembled metallosupramolecular helicates with promising antimicrobial activity have attracted greater interest due to their DNA-binding properties.[13,14] Interestingly, further studies showed that changing the metal centre in the helicate structure influences the bactericidal activity against certain bacterial strains.[15] Despite some promise in these early applications, similar systems were not explored further.

With fast emergence in antibiotic resistance, combined with the decline in novel antibiotic therapies, the need to discover and develop new natural as well as synthetic antibiotic agents has increased significantly. One attractive option is the combination of antimicrobial peptides (AMPs) and metal ions. AMPs are a promising antibiotic class with some structural diversity and broad activity spectrum.[16] Formally, they can also be distinguished in natural (typically with longer peptide sequences and post-synthetic modifications) and synthetic AMPs (synAMPs), the latter typically having shorter sequences, and possibly non-natural modifications.[17,18] One of these modifications can be the covalent modification of peptides with metal complexes to enhance their antimicrobial activity, or alter their spectrum of activity.[2,19,20] The presence of metals could lead to conformational changes in the AMPs followed by change of their properties and biologically activity. In natural

Faculty of Chemistry and Biochemistry, Inorganic Chemistry I – Bioinorganic Chemistry, Ruhr University Bochum, Universitätsstrasse 150, 44780 Bochum, Germany. E-mail: nils.metzler-nolte@rub.de; https://www.chemie.rub.de/ac1

† Electronic supplementary information (ESI) available. See DOI: https://doi.org/10.1039/d4dt00907j

systems, metallopeptides such as bacitracin (isolated from *Bacillus subtilis*), coordinated with several divalent transition metal ions (*e.g.* Zn, Mn, Co and Cu), and bleomycin (isolated from *Streptomyces verticillatus*), coordinated with Cu(II) or Fe (II), showed enhanced biological activity in inhibiting bacterial growth than in their pure form.[21–25] Herein, we report the coordination-driven supramolecular conjugates of cobalt and short cationic peptide derivatives of a known antimicrobial H-$(RW)_3$-NH_2 peptide (Fig. 1). The $(RW)_3$ motif was first reported and its structure–activity relationship (SAR) investigated by Svendsen and coworkers.[26] Numerous modifications of this peptide were investigated, including N-terminal and side chain modification with organometallic complexes and fatty acids, often leading to spectacular activity *e.g.* against cystic fibrosis.[27] Modifications of the $(RW)_3$ peptide with unnatural transition metal complexes like ruthenocene were also crucial to finally elucidate the mode of action of this highly attractive class of synAMPs. This membrane-targeting peptide causes delocalization of peripheral membrane proteins, ultimately limiting cellular energy and undermining cell-wall integrity.[28]

The essential transition metal cobalt (Co) exhibits a unique redox chemistry and is an integral part of the vitamin B_{12} group that is essential for healthy nervous system function, production of red blood cells, and metabolism of folic and fatty acids.[29] Compared to some other transition metals like Pt and Au, the biological activity of cobalt compounds has not been studied in details. There are only a few cobalt-based compounds which exhibit activity against several bacteria and viruses.[30–39] Nagababu *et al.* investigated a series of Co(III) mixed ethylenediamine complexes, which exhibited antibacterial activity against nonpathogenic bacteria. Out of those, the Co complexes with bipyridine, 1,10-phenanthroline, dimethylimidazole, and pyrazole exhibited the highest antibacterial activity.

Further investigation by these authors of the fungicidal properties of these complexes revealed also high antifungal activity.[35] Of relevance for the present work is Co in oxidation states +II (d^7-Co), which is kinetically labile with rapid ligand exchange, and its +III oxidation state (d^6-Co) that supports complexes with similar geometry, but is substitutionally inert.

Characterisation and structural investigation in the field of supramolecular chemistry is always a major challenge, especially in self-organizing systems with potentially multiple stoichiometries. Increasingly, diffusion-ordered NMR spectroscopy (DOSY) is gaining popularity, being used to glean information on the size and shape, as well to probe intermolecular complex formation. For example, diffusion measurement has been successfully applied to characterize the structure of metallosupramolecular helicates and rotaxane, and to study their behaviour in solution.[40,41] Therefore, for the characterization of herein synthesized supramolecular systems the diffusion-ordered NMR spectroscopy (DOSY) is the method of choice. DOSY provides a reasonable approximation for the determination of the possible complex stoichiometry by using the Stokes–Einstein equation (eqn (1)).[42–44] In this work, we report the synthesis of antimicrobial peptides featuring terpyridine (tpy) ligands for metal complexation and the subsequent selective self-assembly of these peptides into 'oxidatively locked' metallosupramolecular architectures using the redox-dependent lability of Co $(tpy)_2$ complex formation. After characterisation of the complexes, including their exact composition and stoichiometry, the influence of stoichiometry and metal presence or absence on antimicrobial activity will be investigated by determining the minimal inhibitory concentration (MIC).

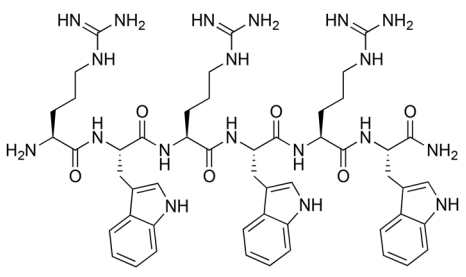

Fig. 1 Structure of the parent H-$(RW)_3$-NH_2 peptide.[6]

Results and discussion

Design strategy

In order to obtain different $(RW)_3$ peptide derivatives with metal-chelating abilities, a new terpyridine-containing amino acid was synthesized. To this end, a carboxylic acid derivative of the metal binding 2,2′:6′,2″-terpyridine (tpy) ligand was coupled to the side-chain amino group of the hydrophilic basic amino acid lysine (Lys), following a modified literature procedure.[45,46] Then, this Lys(tpy) amino acid either substituted the tryptophan (W) of the $(RW)_3$ peptide or was added to the sequence (Fig. 2). Either one or two Lys(tpy) derivatives were incorporated into the sequences to explore structure–activity relationships (SAR). All peptides and peptide-terpyridine derivatives for metal conjugation were prepared by solid phase synthesis techniques.[47] The tpy ligand forms stable bis-complexes with pseudo octahedral coordination at the metal centre with metal ion in low oxidation states.[48] The σ-donor and π-acceptor character of the terpyridine ligands as well as the chelate effect contribute to the complex stability.[49,50] Additionally, both bivalent cobalt and pyridine belong to the borderline group according to Pearson's hard and soft Lewis acids and bases (HSAB) theory.[51] So, the affinity of the metal to the nitrogen atoms of the tpy ligand outcompetes other potential donor atoms in the peptide structure, which leads to a high probability of the desired complex formation. However, because ligands around the kinetically labile Co(II) ion can still rearrange, the preferred $Co(tpy)_2$ product was subsequently "locked" by oxidation of the metal ion to the inert Co(III) oxidation state.

Synthesis

The peptide synthesis was performed manually at room temperature using an fluorenylmethyloxycarbonyl (Fmoc) protection

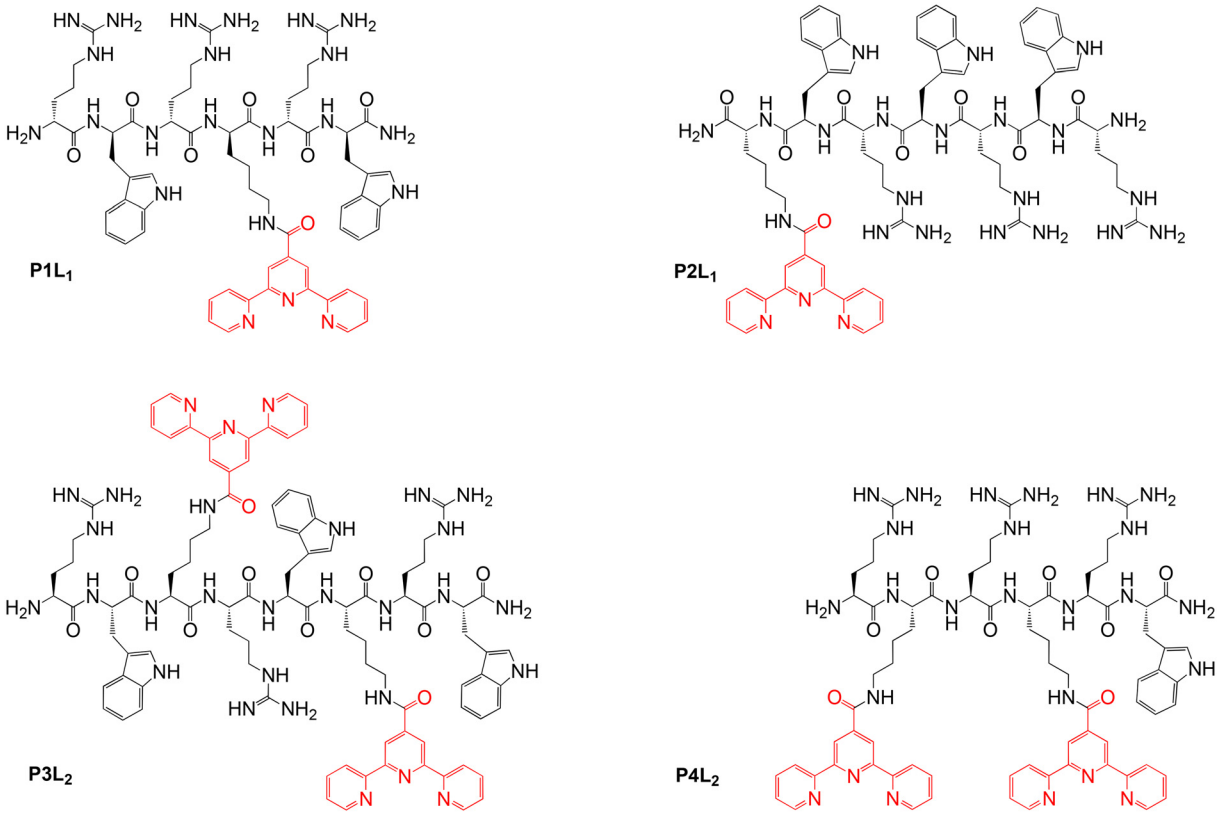

Fig. 2 Overview of the isolated peptides (P1–P4) coupled with tpy ligands (L_n, n = 1,2 Lys(tpy) residues).

strategy on Rink amide resin as solid support. The coupling reaction of amino acids was carried out by using the coupling reagent 2-(1*H*-benzotriazole-1-yl)-1,1,3,3-tetramethyluronium tetrafluoroborate (TBTU) and the additional base diisopropylethylamine (DIPEA) in excess (see ESI† for details).[46] The further attachment of the ligands on the peptides was also carried out on the solid support. For that purpose, Lys with the *tert*-butyloxycarbonyl (Boc) protecting group on the side chain was chosen, because of deprotection condition with low concentrated trifluoroacetic acid (TFA) solution (30%). By contrast, the peptide cleavage from the Rink amide resin and deprotection of arginine and tryptophan side chains require a higher concentration of TFA (95%).[52] Thus, coupling of terpyridine carboxylic acid to the lysine amino side chain could be carried out selectively, minimizing the formation of undesired by-products. The tpy ligand was attached to the Lys side chain on the solid phase using a coupling reagent mixture of diisopropylcarbodiimide (DIC) and hydroxybenzotriazole (HOBt). Isolation and purification of the tpy-derivatized peptides after cleavage from the Rink amide resin was performed by semi-preparative reverse phase HPLC followed by lyophilisation. Analytical data of the peptides are summarized in Table 1, with structures shown in Fig. 2.

The cobalt peptides conjugates are made by one pot reaction of a 2 : 1 : 1 or 1 : 1 : 1 ratio of prepared peptides, $Co^{II}(BF_4)_2{\cdot}6H_2O$ and later oxidizing agent $NH_4[Ce^{IV}(NO_3)_6]$, in DMSO-d^6 (Table 2). Formation of the complexes was accompanied by a colour change. After addition of the purple solution of high-spin Co(II) complex to the colourless peptide solution, product formation was accompanied by the immediate change to dark red orange colour. After chemical oxidation to the more stable Co(III)-peptide complexes by Cer(IV) salt, a

Table 1 Analytical data of the purified peptides (P1–P4) coupled with tpy-ligand (L)

Peptide	Calcd Mass [*M*] (g mol^{-1})	MS MALDI-TOF [M + H]$^+$	Retention time HPLC (min)	Diffusion coefficient in DMSO-d^6 (m^2 sec^{-1})	Yield after purification *via* HPLC (%)
$P1L_1$	1244.66	1245.75	7.2	8.81×10^{-11}	4
$P2L_1$	1430.74	1431.7	7.4	8.5×10^{-11}	4
$P3L_2$	1817.91	1818.17	5.6	7.78×10^{-11}	3
$P4L_2$	1445.75	1446.91	5.4	7.86×10^{-11}	7

Table 2 Analytical data of the isolated Cobalt peptide conjugates ($[Co^{III}(P1L_1)_2]^{3+}$, $[Co^{III}(P2L_1)_2]^{3+}$, $[(Co^{III}(P3L_2))_2]^{6+}$, $[(Co^{III}(P4L_2))_2]^{6+}$)

Co-peptide conjugates	Calcd mass [M] (g mol^{-1})	MS MALDI-TOF	Diffusion coefficient in DMSO-d^6 (m^2 sec^{-1})	Yield (%)
$[Co^{III}(P1L_1)_2]^{3+}$	2548.25	1303.84 $[Co^{III}(P1L_1)]^+$; 1245.88 $[P1L_1 + H]^+$	6.42×10^{-11}	90
$[Co^{III}(P2L_1)_2]^{3+}$	2920.14	1489.37 $[Co^{III}(P2L_1)]^+$; 1431.8 $[P2L_1 + H]^+$	6.14×10^{-11}	93
$[(Co^{III}(P3L_2))_2]^{6+}$	3753.68	1935.07 $[Co_2{}^{III}(P3L_2)]^+$; 1876.15 $[Co^{III}(P3L_2) + H]^+$; 1818.15 $[P3L_2 + H]^+$	5.42×10^{-11}	90
$[(Co^{III}(P4L_2))_2]^{6+}$	3009.36	1563.7 $[Co_2{}^{III}(P4L_2)]^+$; 1505.05 $[Co^{III}(P4L_2) + H]^+$; 1446.97 $[P4L_2 + H]^+$	5.56×10^{-11}	92

second colour change to pale orange was observed (for more details, including electronic absorption spectra, see ESI†). Reactions were carried out in deuterated DMSO to enable NMR monitoring of the reaction progress, however products were later isolated by precipitation (see ESI† for exact procedure). The schematic formation of cobalt-peptide conjugates is presented in Scheme 1.

In order to verify the correct binding of the cobalt to the nitrogen of terpyridine ligands in the peptide structure, product formation was monitored by higher frequency (400 MHz) ^{1}H-NMR. The first spectrum was made after the peptide-ligand synthesis, then after the Co^{II}-complex formation, and then again after oxidation by Cer(IV). The characteristic terpyridine signals in the ^{1}H-NMR spectrum of $P1L_1$ were identified by comparison with the ^{1}H-NMR spectrum of 2,2′:6′,2″-terpyridine-4′-carboxylic acid (L) (Fig. 3).

From the ^{1}H NMR spectra in Fig. 3, it can be seen that the aromatic protons of the tpy ligand (8.5 ppm to 9 ppm) were broadened and shifted to low field in the spectrum of the Co(II)-complex, consistent with coordination to a paramagnetic metal centre.[23] After oxidation to Co(III), the paramagnetic effect vanished, which led to the absence of signals in the low field and increased the quality of the spectrum (Fig. 3, top, purple). However, the tpy signals remained shifted in the spectrum of the Co(III)-peptide complex. To ensure the correct coordination of the peptide to cobalt, a higher frequency ^{1}H

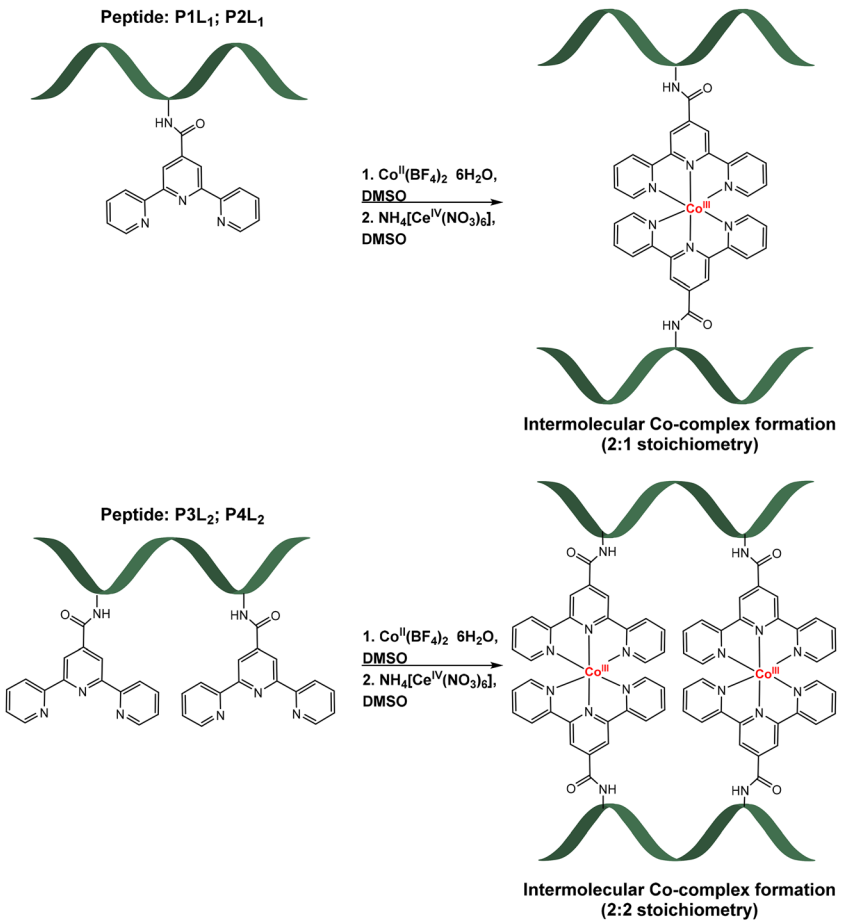

Scheme 1 Formation of Co-peptide conjugates with one tpy ligand (top, $[Co^{III}(P1L_1)_2]^{3+}$; $[Co^{III}(P2L_1)_2]^{3+}$) and two tpy ligands (bottom, $[(Co^{III}(P3L_2))_2]^{6+}$; $[(Co^{III}(P4L_2))_2]^{6+}$).

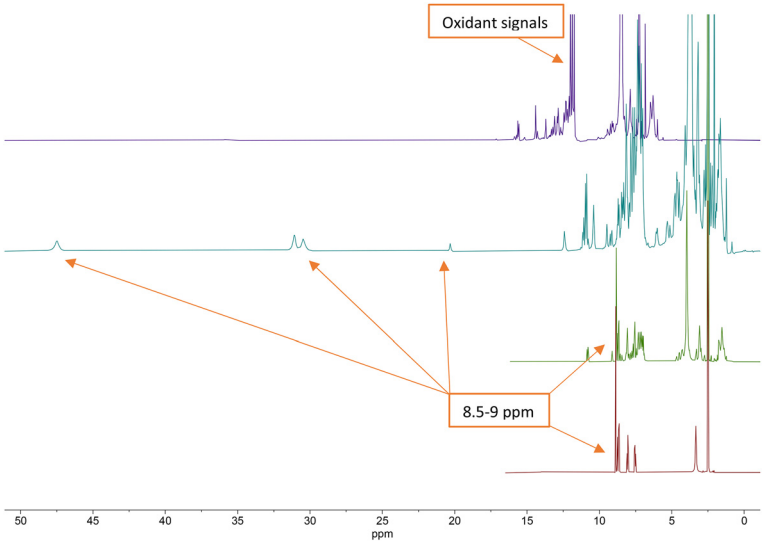

Fig. 3 Stacked ^{1}H NMR (400 MHz) spectra of terpyridine ligand (bottom, red), $P1L_1$ (middle, green), $[Co^{II}(P1L_1)_2]^{2+}$ complex (middle, teal) and $[Co^{III}(P1L_1)_2]^{3+}$ complex (top, purple).

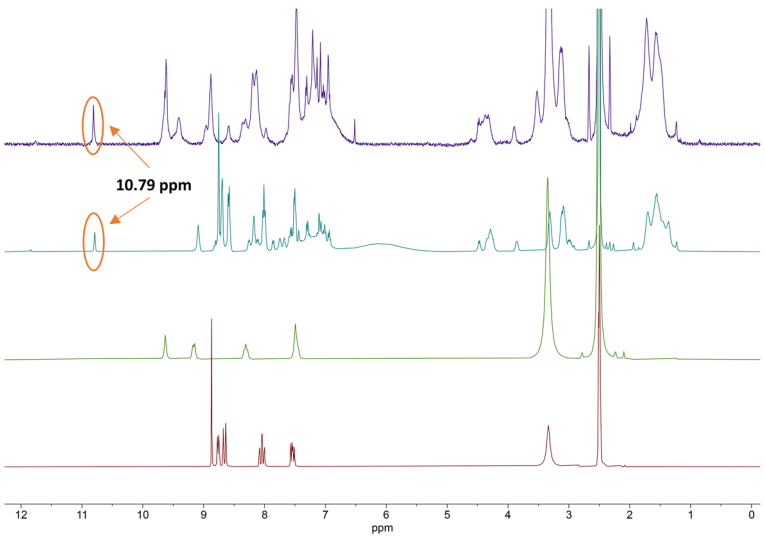

Fig. 4 Stacked ^{1}H NMR (700 MHz) spectra of terpyridine ligand (tpy-COOH, bottom, red), $[Co^{III}(tpy\text{-}COOH)_2]^{3+}$ (middle, green), $P4L_2$ (middle, teal) and $[(Co^{III}(P4L_2))_2]^{6+}$ complex (top, purple).

NMR (700 MHz) was recorded (Fig. 4). In the stacked spectra, the characteristic terpyridine ligand signals at 7.5 ppm, 8.0 ppm, and 8.5 ppm to 9.0 ppm (Fig. 4, red spectrum) appeared in the ^{1}H NMR of $P4L_2$ with a slight shift to the higher field (Fig. 4, teal spectrum). After complexation and oxidation to Co(III), the terpyridine signals could be approximately assigned in the ^{1}H NMR spectrum (Fig. 4, top, purple spectrum) if compare with the ^{1}H NMR of tpy-Co(III) complex (Fig. 4, middle green spectrum). However, the NH-proton of the indole remained at 10.79 ppm in both spectra, in $P4L_2$ and Co(III)-$P4L_2$; therefore, it can be assumed that the tpy ligand was coordinated to the cobalt ion.

To purify the final product from ceric ammonium nitrate, precipitation with ethyl acetate/diethyl ether (1 : 1) and lyophilization was carried out. The ^{1}H-NMR spectrum confirmed the absence of the oxidant, since ceric ammonium nitrate has characteristic signals in the range between 6.9 ppm and 7.2 ppm (for more details see ESI,† including assignment of ^{1}H NMR signals).

Characterization of the cobalt-peptide conjugates

The previous investigation of the formation of the cobalt peptide conjugates using ^{1}H NMR (Fig. 3 and 4) has demonstrated that cobalt is coordinated to the terpyridine ligands. To

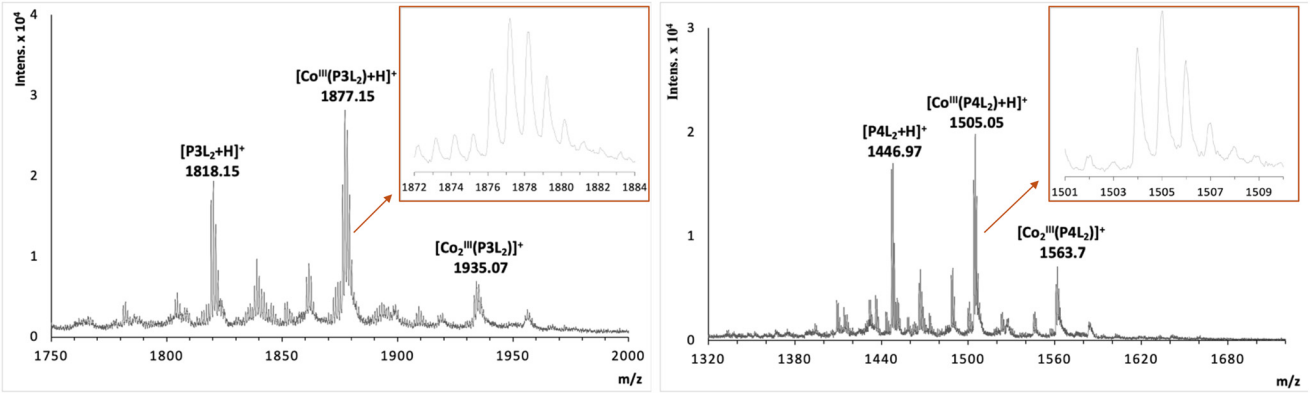

Fig. 5 MALDI TOF spectrum of cobalt-peptide conjugate $[(Co^{III}(P3L_2))_2]^{6+}$ (left) and $[(Co^{III}(P4L_2))_2]^{6+}$ (right). Note that all peaks in the mass spetra are singly charged (as proven by the peak distance of isotopomers in the inserts); this is a consequence of the ionization technique rather than a molecular property.

investigate and possibly confirm the predicted 2 : 1 stoichiometry of the formed supramolecular complexes with peptides $P1L_1$ and $P2L_1$, and the 2 : 2 stoichiometry of complex formation for peptides with two tpy ligands ($P3L_2$ and $P4L_2$), mass spectrometry measurements were performed using MALDI TOF (see suppl. information for mass spectra of all complexes). For the cobalt conjugates with two tpy entities the masses of characteristic fragments were detected, such as 1935.07 for $[Co_2^{III}(P3L_2)]^+$ and 1563.7 for $[Co_2^{III}(P4L_2)]^+$, respectively (Fig. 5). The presence of peaks originating from fragments with two metal centres and one peptide entity rules out intramolecular complex formation (*i.e.* two tpy ligands from the same peptide binding one Co center) and rather suggests intermolecular complex formation as indicated in Scheme 1 (bottom). However, these mass spectrometry results could only be taken as a first indication and further studies are required to confirm the preferred stoichiometry of the complexes formed (see Scheme 2, and discussion below).

The detected masses for the cobalt complexes with peptides $P1L_1$ and $P2L_1$ correspond to fragments with one peptide unit and one cobalt centre (see ESI†), 1303.84 for $[Co^{III}(P1L_1)]^+$ and 1489.37 for $[Co^{III}(P2L_1)]^+$, respectively. Unfortunately, characterization of the Co conjugates by HPLC was impossible. After HPLC purification of the cobalt conjugates, only the peptides could be isolated, indicating the instability of the complexes under HPLC conditions. To further verify the purity and confirm the predicted stoichiometry of the formed complexes, the diffusion-ordered NMR spectroscopy (DOSY NMR) was applied (Fig. 6 and 7, for more spectra see ESI†).

The DOSY spectral results demonstrate that the complexation reaction with cobalt led to the clean formation of only one product. Since each species has a different diffusion coefficient in the solvent, they move at different rates and therefore appear on different horizontal levels of a 2D DOSY NMR spectrum. This can be observed in the stacked DOSY NMR spectra of the metal-free peptides $P2L_1$ and $P4L_2$ (Fig. 6 and 7, green), which has a greater diffusion coefficient than its cobalt conjugates (Fig. 6 and 7, red) because of the faster movement in the solvent. Since no respective signals of metal-free peptides in the 2D DOSY NMR spectrum of cobalt complexes were observed, it can be assumed that the reaction proceeds to completion.

The ligand-to-metal ratio (stoichiometry) by the complex formation can vary due to different factors (*e.g.* reduction of entropy, sterically influence, affinity of the metal centre to other donor atoms within the peptide structure), these lead to differences in the size of the molecules, which in turn leads to differences in the rate of diffusion in the solution. In this case, the observed diffusion coefficients from the DOSY NMR experiments were used to calculate the hydrodynamic size of the prepared compounds with the aim of determining the stoichiometry of the complexes (Schemes 1 and 2). Since the observed diffusion coefficients of the complexes are lower than the diffusion coefficients of the peptides, it can be assumed that the formed cobalt conjugates are larger and move slower in the solution than the peptides. Diffusion coefficients (D) were reported in DMSO-d^6 for each individual signal and were averaged to obtain molecular diffusion coefficients for the metal-free peptides and the cobalt conjugates, respectively. Then, the Stokes radius as well as a spherical volume ($V = \frac{4}{3}\pi r^3$) of the molecules using the Stokes–Einstein equation (eqn (1)) were calculated (Table 3).

$$D = \frac{k_B T}{6\pi\eta r_s} \quad (1)$$

In eqn (1), k_B is the Boltzmann constant, η is the viscosity of the solvent in which diffusion occurs at temperature T (for DMSO η = 1.996 Pa s at 293 K), and r_s is the Stokes radius of the diffusing species. The following calculation of the volume ratios of cobalt-free peptides and Co-peptide conjugates allows the prediction of the complex stoichiometry.

As can be seen in Table 3, the calculated values of the volume ratios of peptides with one tpy entity to their cobalt complexes are greater than two, which means that two peptides coordinate to one cobalt centre and therefore the stoi-

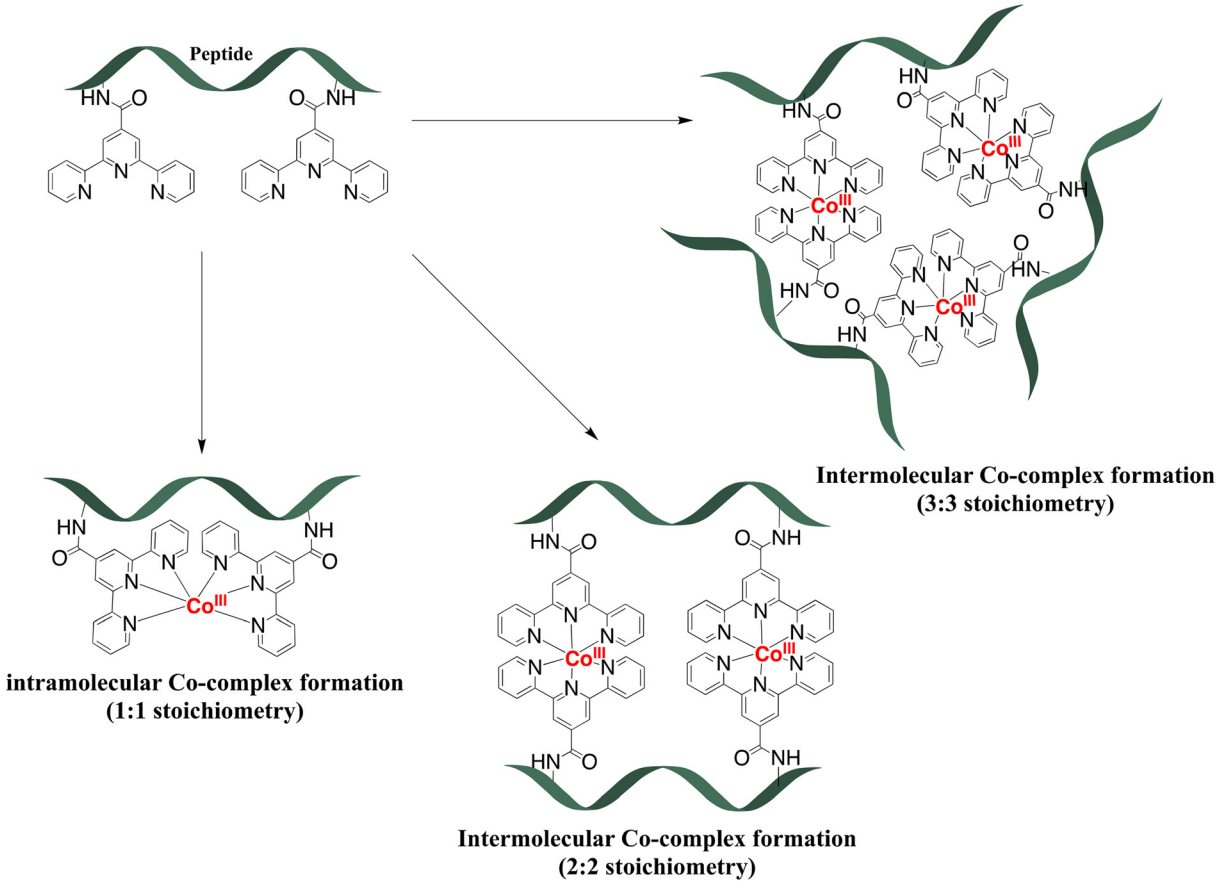

Scheme 2 Possible stoichiometry of complexes during the coordination of peptides with two tpy ligands ($P3L_2$ and $P4L_2$) to the cobalt ion.

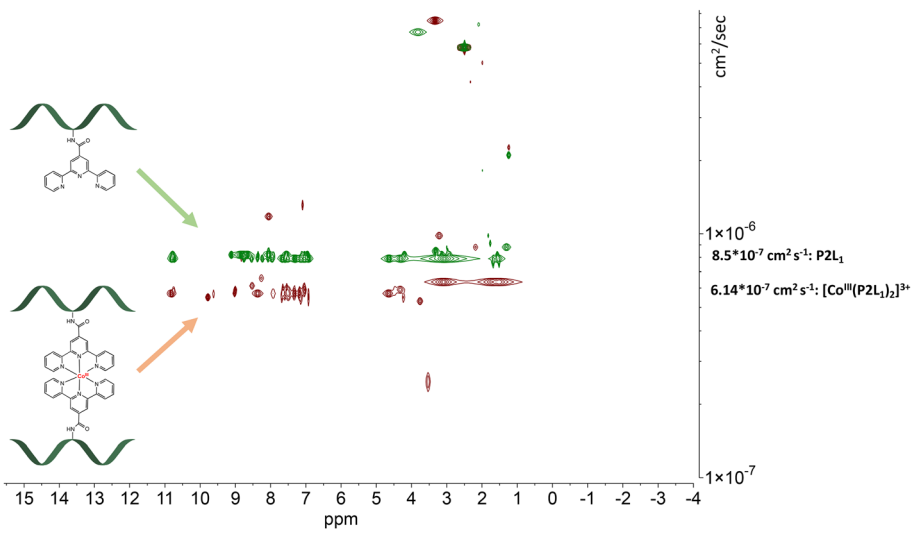

Fig. 6 Stacked DOSY NMR spectrum of $P2L_1$ (green) and $[Co^{III}(P2L_1)]^{3+}$(red) directly after the oxidation reaction in DMSO-d^6 (2.50 ppm), water peak is at 3.33 ppm.

chiometry of the complex is 2 : 1 (Scheme 1). Ideally, this volume ratio would be approximately two, if it is assumed that the structure of the molecules is a hard sphere moving in a continuum fluid without any external contributions by solvation or other interactions. However, a deviation from the ideal value can be expected. A study by Allouche *et al.* demonstrated that the calculated hydrodynamic radius by the modification of the Stokes–Einstein equation for non-spherical

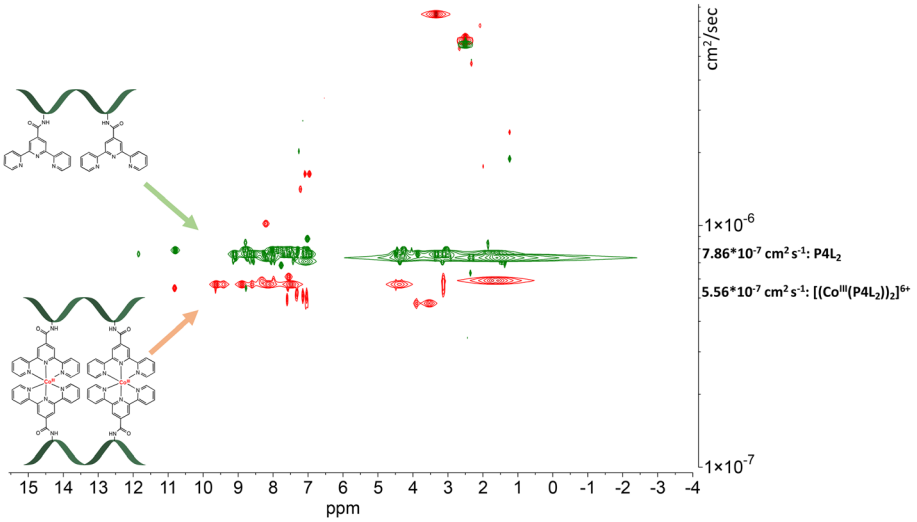

Fig. 7 Stacked DOSY NMR spectrum of $P4L_2$ (green) and $[(Co^{III}(P4L_2))_2]^{6+}$ (red) directly after the oxidation reaction in DMSO-d^6 (2.50 ppm), water peak is at 3.33 ppm.

Table 3 Results from the DOSY NMR experiments of peptides, and their Co(III) conjugates

Peptides and their cobalt conjugates	Calcd mass (g mol^{-1})	$D_{(average)}$ (m^2 sec^{-1})	Stokes radius (Angstrom, Å)	Volume (Å^3)	$\frac{V_{Co\text{-}peptide}}{V_{peptide}}$
$P1L_1$	1244.66	8.81	12.2	7590	**2.58**
$[Co^{III}(P1L_1)_2]^{3+}$	2548.25	6.42	16.7	19 629	
$P2L_1$	1430.77	8.5	12.6	8469	**2.66**
$[Co^{III}(P2L_1)_2]^{3+}$	2920.14	6.14	17.5	22 516	
$P3L_2$	1817.91	7.78	13.8	11 050	**2.95**
$[(Co^{III}(P3L_2))_2]^{6+}$	3753.68	5.42	19.8	32 634	
$P4L_2$	1445.75	7.86	13.7	10 683	**2.83**
$[(Co^{III}(P4L_2))_2]^{6+}$	3009.36	5.56	19.34	30 317	

species has an approximately similar deviation from the hydrodynamic size (r_s) calculated by the general eqn (1) for different non-spherical molecules.[53] Therefore, it was confirmed that the Stokes–Einstein approximation is also valid for non-spherical molecules and the derived hydrodynamic size can also be applied for further investigation of molecular systems. The observed deviation of the volume ratio from the ideal ratio can be explained not only by the non-spherical structure of the prepared compounds, but also by the high charge, which is distributed over the whole system, due to the presence of the basic amino acid arginine and the trivalent metal centre. Each positive charge requires an associated anion, which is TFA^- or BF_4^- in the case of the compounds prepared herein. These anions do not diffuse completely independently and therefore contribute to the measured volume. Additionally, a higher charge on the whole molecules leads to the stronger solvation, which in turn leads to the reduction of the diffusion rate. A slight contribution of peptide size to the diffusion coefficient of the peptides and their cobalt conjugates is even detected between very similar compounds of one stoichiometry, *e.g.* of the CoL_2 type. Peptide $P2L_1$ has seven amino acids in its structure and $P1L_1$ only six, and consequently diffusion of $P1L_1$ (and its Co complex) is slightly faster than $P2L_1$ (compare entries 1 *vs.* 3, and 2 *vs.* 4 in Table 3). For peptides with two tpy entities, the size effect is more remarkable, as can be seen by the fact that both $P1L_1$ and $P4L_2$ are six amino acid peptides, but $P4L_2$ has two lysine residues and a significantly larger Stokes volume (Table 3).

For the determination of the expected 2 : 2 stoichiometry of the conjugates with two tpy entities ($P3L_2$ and $P4L_2$), the same calculation as previous was made (Scheme 2 and Table 3). The observed volume ratio is only slightly greater than the volume ratio of the peptides with one tpy entity and 2 : 1 stoichiometry (compare $[Co^{III}(P1L_1)_2]^{3+}$ and $[(Co^{III}(P4L_2))_2]^{6+}$ for peptides with identical number of amino acids). The reason is very likely the second Co(III) centre, which increases the overall charge of the structure. Furthermore, more tpy entities in the structure of peptides and their cobalt conjugates, as well as more amino acids in case of $P3L_2$ also contribute to a higher molecular weight, but likely also to a greater deviation from the ideal spherical shape.

Potentially, a number of other structures are conceivable especially for $P3L_2$ and $P4L_2$ peptides with more than one tpy ligand on the peptide backbone, some of which are shown in Scheme 2. First, if formation of an intramolecular Co-complex with 1 : 1 stoichiometry would have occurred (which might be

considered entropically favourable), then it would be expected to have a much greater diffusion coefficient due to the smaller size of the molecules. Additionally, during MALDI TOF measurement the mass of the fragment containing only one cobalt and one peptide should be detected, as in the case of cobalt conjugates of $P1L_1$ and $P2L_1$ (Table 2). Neither DOSY nor mass spectra gave a hint to this 1 : 1 stoichiometry, indicating that intramolecular complex formation does not occur. Possibly, it might be sterically hindered due to the close proximity of the terpyridine entities on the peptide. By contrast, the 3 : 3 stoichiometry of the complex (Scheme 2) would result in a supramolecular complex with a higher molecular weight. Such a molecule would have a much lower diffusion coefficient and higher volume ratio (in comparison to the two 2 : 2 complexes) – which again was not observed in our DOSY experiments. Additionally, such complexes with a higher ligand-to-cobalt ratio are entropically unfavorable.[54] Therefore, from the existing MS and 2D DOSY NMR data we conclude that $P3L_2$ and $P4L_2$ both form exclusively intermolecular Co complexes with 2 : 2 stoichiometry.

Influence of metal centre and complex stoichiometry on antimicrobial activity of the peptides

Determination of the minimum inhibitory concentration (MIC) is usually a starting point for more extensive preclinical evaluation of tested antibacterial substances. The MIC value represents the lowest concentration of antimicrobial agents required for visible hindrance of bacterial growth *in vitro*. The determination of the MIC values was performed as described by Albada *et al.*,[55,56] see experimental section for a detailed description of procedures and Table 4 for results. The MIC data were used in this work to investigate the changes in antimicrobial activity of peptides upon coordination to the cobalt ions. For the calculation of the MIC values in μM, the molecular weights of the peptides together with one TFA counter ion for each basic amino acid residue were used. The molecular weight of the cobalt-peptide conjugates was calculated together with BF_4 counter ions.

By comparing the observed biological results, it can be concluded that not only double peptide entities in the structure of conjugates but also the complexation with cobalt increases the activity of peptides almost in every case. By and large, peptides and their Co complexes are more active against Gram-positive bacteria than against Gram-negative ones. Importantly however, peptides $P1L_1$ and $P2L_1$ demonstrate higher activity against Gram-negative pathogens upon complexation with cobalt. The obtained values are even smaller than the MIC of the parent $(RW)_3$ peptide against *E. coli*, *A baumannii*, and *P. aeruginosa*. Within the range of peptide-ligand structures tested herein, the greatest activity against Gram-negative pathogens is found for $[Co^{III}(P2L_1)_2]^{3+}$. For instance, introduction of cobalt through the formation of an octahedral complex with two tpy ligands attached on the lysine residue of $P1L_1$ and $P2L_1$ increases the activity against *E. coli* twofold (considering that the cobalt complexes contain two bactericidal peptide units). In contrast, the peptides $P3L_2$ and $P4L_2$ with two tpy ligands each demonstrate low activity against Gram-negative pathogens, and complexation to cobalt does not make a significant difference. In the case of Gram-positive pathogens (two *S. aureus* strains, including the multi-resistant ATCC 43300 strain), the greatest activity (7.6 μM) is observed for $[(Co^{III}(P4L_2))_2]^{6+}$. Again, this is approximately twofold greater than the activity of the cobalt-free peptide $P4L_2$ (considering that $[(Co^{III}(P4L_2))_2]^{6+}$ has two peptides in its structure). This activity matches that of the parent $(RW)_3$ peptide against the same *S. aureus* strains, with 11 μM and 6 μM, respectively.

As one would expect, exchanging Trp for Lys(tpy) influences the activity of the metal-free peptides, but not in a uniform way. Exchanging one or more Trp residues strongly decreases activity of the peptide against Gram-positive bacteria. Surprisingly however, $P1L_1$ and $P2L_1$ with only one Lys(tpy) moiety instead of Trp in their structures, are less active against *S. aureus* strains than $P4L_2$ with two Trp exchanged against Lys

Table 4 Minimum inhibitory concentration (MIC in μM) of peptides containing tpy-ligand and cobalt conjugates of these peptides against several clinically relevant isolates of Gram-positive and Gram-negative bacteria (incubation time: 16 h at 37 °C, culture media: Mueller Hinton broth and Mueller Hinton II broth for *P. aeruginosa*)

	Minimal inhibitory concentration (μmol l^{-1})						
	Gram −			Gram +			Yeast
Peptides and their cobalt conjugates	*E. coli* DSM 30083	*A. baumannii* DSM 30007	*P. aeruginosa* DSM 50071	*B. subtilis* 168 DSM402	*S. aureus* DSM 20231	*S. aureus* ATCC 43300	*C. albicans* DSM1386
$(RW)_3$	21	85	>100	3	11	6	—
$P1L_1$	75.2	>75.2	>75.2	9.4	>75.2	>75.2	18.8
$[Co^{III}(P1L_1)_2]^{3+}$	18.3	18.3	>146.1	9.1	36.5	18.3	4.6
$P2L_1$	67.8	>67.8	67.8	33.9	67.8	67.8	16.9
$[Co^{III}(P2L_1)_2]^{3+}$	16.5	33	66	8.2	33	16.3	4.1
$P3L_1$	>56.3	>56.3	>56.3	7	>56.3	>56.3	14.1
$[(Co^{III}(P3L_2))_2]^{6+}$	>51.5	>51.5	>51.5	25.7	51.5	51.5	51.5
$P4L_2$	134.5	67.3	67.3	33.6	33.6	33.6	4.2
$[(Co^{III}(P4L_2))_2]^{6+}$	>60.6	>60.6	>60.6	7.6	7.6	7.6	7.6
$[Co^{III}\text{-}(tpy\text{-}COOH)_2]^{3+}$	>292.9	>292.9	>292.9	>292.9	>292.9	>292.9	>292.9

(tpy) moieties. On the other hand, $(RW)_3$ has low activity against any Gram-negative strain, and swapping Trp for Lys (tpy) makes very little difference overall. It is also interesting to note that the compounds exhibit a peculiar bactericidal behaviour against the Gram-positive bacterium *B. subtilis*. For example, the presence of cobalt in the $P1L_1$ structure has only a slight influence on the activity, while adding cobalt to peptides $P4L_2$ and $P2L_1$ significantly increases the activity. In the case of $P3L_2$, the bactericidal activity even decreases threefold through the insertion of cobalt. It remains for future experiments to determine whether these remarkably non-uniform tendencies are determined by the hydrophobic character, modified membrane interactions due to less Trp residues, or simply a consequence of differential bacterial uptake in the different species.

Remarkably, minimum inhibitory concentrations against the opportunistic pathogenic yeast *C. albicans* range between 4.13 μM and 51.5 μM, thereby indicating a potent antimicrobial activity of peptides and their cobalt conjugates. The greatest activity against *C. albicans* was observed for $[Co^{III}(P2L_1)_2]^{3+}$ (4.1 μM), which overall exhibits the best broadband activity across all tested pathogens. Again, the insertion of cobalt also reduces the activity of $P3L_2$, as in the case of Gram-positive *B. subtilis*, making it less active than the metal-free peptide. Finally, the $[Co^{III}(tpy\text{-}COOH)_2]^{3+}$ complex is not active against any of the tested bacteria and yeast (MIC values > 293 μM), thereby ruling out an activity of the $Co(tpy)_2$ complex, or the metal ion itself after decomplexation.

Conclusion

In this work, the synthesis of four new antimicrobial peptides featuring terpyridine ligands as metal binding sites was achieved. Addition of $[Co^{II}(H_2O)](BF_4)_2$ resulted in self-assembly to selectively form L_2M and L_4M_2 bioconjugates, depending on the number of tpy ligands on the peptide. The intended complex formation and stoichiometry could be confirmed by MALDI-TOF mass spectrometry. Further characterisation by DOSY NMR experiment showed the purity of the conjugates and indicated the intermolecular complex formation based on the obtained diffusion coefficients. Preliminary biological tests (determination of minimum inhibitory concentration) of the cobalt-peptide conjugates showed that the complexation increased almost in every case the antimicrobial activity of peptides. Interestingly, the presence of cobalt ion in the structure of $P1L_1$ and $P2L_1$ increased activity against *E. coli*, *S. aureus* ATCC 43300, yeast *C. albicans and B. subtilis* 168 DSM402 in case of $P1L_1$ twofold (considering that in the cobalt complexes are two bactericidal peptide units). The greatest activity against *C. albicans* was observed for $[Co^{III}(P2L_1)_2]^{3+}$ (4.1 μM).

Future research will focus on further biological tests to understand the bactericidal role of cobalt ion in the structure of peptides. Since the mode of action of $(RW)_3$ peptide is well studied, the proteomic profiling of synthesized conjugates can provide the information about the influence of cobalt ion on mechanism of action of peptides.

Author contributions

L. J.: investigation, visualization, writing – original draft; R. G. M.: supervision, writing – review and editing; N. M.-N.: conceptualization, supervision, funding acquisition, writing – review and editing.

Conflicts of interest

The authors declare no conflict of interest.

Acknowledgements

The authors are grateful to Pascal Dietze and Prof. Dr Julia Bandow for the Measurement of minimal inhibitory concentration (MIC) of isolated peptides and their cobalt conjugates. R. G. M. is grateful to the Alexander von Humboldt Foundation for a postdoctoral fellowship.

References

1 J. W. Alexander, *Surg. Infect.*, 2009, **10**, 289–292.
2 B. Albada and N. Metzler-Nolte, *Acc. Chem. Res.*, 2017, **50**, 2510–2518.
3 J. Liang, D. Sun, Y. Yang, M. Li, H. Li and L. Chen, *Eur. J. Med. Chem.*, 2021, **224**, 113696.
4 A. Evans and K. A. Kavanagh, *J. Med. Microbiol.*, 2021, **70**, 001363.
5 P. Biegański, Ł. Szczupak, M. Arruebo and K. Kowalski, *RSC Chem. Biol.*, 2021, **2**, 368–386.
6 A. Frei, J. Zuegg, A. G. Elliott, M. Baker, S. Braese, C. Brown, F. Chen, C. G. Dowson, G. Dujardin, N. Jung, A. P. King, A. M. Mansour, M. Massi, J. Moat, H. A. Mohamed, A. K. Renfrew, P. J. Rutledge, P. J. Sadler, M. H. Todd, C. E. Willans, J. J. Wilson, M. A. Cooper and M. A. T. Blaskovich, *Chem. Sci.*, 2020, **11**, 2627–2639.
7 Y. Lin, H. Betts, S. Keller, K. Cariou and G. Gasser, *Chem. Soc. Rev.*, 2021, **50**, 10346–10402.
8 A. Pandey and E. Boros, *Chem. – Eur. J.*, 2021, **27**, 7340–7350.
9 M. Claudel, J. V. Schwarte and K. M. Fromm, *Chemistry*, 2020, **2**, 849–899.
10 Y. Kaneko, M. Thoendel, O. Olakanmi, B. E. Britigan and P. K. Singh, *J. Clin. Invest.*, 2007, **117**, 877–888.
11 L. Macomber and J. A. Imlay, *Proc. Natl. Acad. Sci. U. S. A.*, 2009, **106**, 8344–8349.
12 J. B. Wright, K. Lam and R. E. Burrell, *Am. J. Infect. Control*, 1998, **26**, 572–577.
13 L. J. Childs, J. Malina, B. E. Rolfsnes, M. Pascu, M. J. Prieto, M. J. Broome, P. M. Rodger, E. Sletten,

V. Moreno, A. Rodger and M. J. Hannon, *Chem. – Eur. J.*, 2006, **12**, 4919–4927.
14 A. D. Richards, A. Rodger, M. J. Hannon and A. Bolhuis, *Int. J. Antimicrob. Agents*, 2009, **33**, 469–472.
15 S. V. Kumar, W. K. C. Lo, H. J. L. Brooks and J. D. Crowley, *Inorg. Chim. Acta*, 2015, **425**, 1–6.
16 K. V. R. Reddy, R. D. Yedery and C. Aranha, *Int. J. Antimicrob. Agents*, 2004, **24**, 536–547.
17 M. Zasloff, *Nature*, 2002, **415**, 389–395.
18 E. F. Haney, S. C. Mansour and R. E. W. Hancock, in *Antimicrobial Peptides*, ed. P. R. Hansen, Springer New York, New York, NY, 2017, vol. 1548, pp. 3–22.
19 B. Albada and N. Metzler-Nolte, *Chem. Rev.*, 2016, **116**, 11797–11839.
20 H. B. Albada, A.-I. Chiriac, M. Wenzel, M. Penkova, J. E. Bandow, H.-G. Sahl and N. Metzler-Nolte, *Beilstein J. Org. Chem.*, 2012, **8**, 1753–1764.
21 E. G. Seebauer, E. P. Duliba, D. A. Scogin, R. B. Gennis and R. L. Belford, *J. Am. Chem. Soc.*, 1983, **105**, 4926–4929.
22 S. Rao and G. Venkateswerlu, *Curr. Microbiol.*, 1989, **19**, 253–258.
23 L.-J. Ming and J. D. Epperson, *J. Inorg. Biochem.*, 2002, **91**, 46–58.
24 J. T. Garbutt, A. L. Morehouse and A. M. Hanson, *J. Agric. Food Chem.*, 1961, **9**, 285–289.
25 Y. Sugiura, *Biochem. Biophys. Res. Commun.*, 1979, **90**, 375–383.
26 M. B. Strøm, B. E. Haug, M. L. Skar, W. Stensen, T. Stiberg and J. S. Svendsen, *J. Med. Chem.*, 2003, **46**, 1567–1570.
27 R. A. Murphy, M. Coates, S. Thrane, A. Sabnis, J. Harrison, S. Schelenz, A. M. Edwards, T. Vorup-Jensen and J. C. Davies, *Microbiol. Spectrum*, 2022, **10**, e00813–e00822.
28 M. Wenzel, A. I. Chiriac, A. Otto, D. Zweytick, C. May, C. Schumacher, R. Gust, H. B. Albada, M. Penkova, U. Kramer, R. Erdmann, N. Metzler-Nolte, S. K. Straus, E. Bremer, D. Becher, H. Brotz-Oesterhelt, H.-G. Sahl and J. E. Bandow, *Proc. Natl. Acad. Sci. U. S. A.*, 2014, **111**, E1409–E1418.
29 R. Banerjee and S. W. Ragsdale, *Annu. Rev. Biochem.*, 2003, **72**, 209–247.
30 A. Abebe, Y. Bayeh, M. Belay, T. Gebretsadik, M. Thomas and W. Linert, *Future J. Pharm. Sci.*, 2020, **6**, 13.
31 M. N. Akhtar, W. T. A. Harrison, M. Shahid, I.-U. Khan, E. Iqbal and J. Iqbal, *Transition Met. Chem.*, 2016, **41**, 325–330.
32 E. L. Chang, C. Simmers and D. A. Knight, *Pharmaceuticals*, 2010, **3**, 1711–1728.
33 Z. H. Chohan, A. Rauf, S. Noreen, A. Scozzafava and C. T. Supuran, *J. Enzyme Inhib. Med. Chem.*, 2002, **17**, 101–106.
34 J. T. P. Matshwele, S. Odisitse, O. Mazimba, T. B. Demissie, M. O. Koobotse, D. T. Mapolelo, K. Bati, L. G. Julius, D. O. Nkwe, M. Jongman and F. M. Nareetsile, *Inorg. Chim. Acta*, 2024, **563**, 121911.
35 P. Nagababu, J. N. L. Latha, P. Pallavi, S. Harish and S. Satyanarayana, *Can. J. Microbiol.*, 2006, **52**, 1247–1254.
36 M. Patel, M. Chhasatia and B. Bhatt, *Med. Chem. Res.*, 2011, **20**, 220–230.
37 N. Şahin, E. Üstün, İ. Özdemir, S. Günal, N. Özdemir, H. Bülbül, N. Gürbüz, İ. Özdemir and D. Sémeril, *Inorg. Chem. Commun.*, 2023, **157**, 111396.
38 A. Rambabu, N. Ganji and S. Daravath, *J. Fluoresc.*, 2020, **30**, 1397–1410.
39 S. A. Khan, S. A. A. Nami, S. A. Bhat, A. Kareem and N. Nishat, *Microb. Pathog.*, 2017, **110**, 414–425.
40 L. Allouche, A. Marquis and J. Lehn, *Chem. – Eur. J.*, 2006, **12**, 7520–7525.
41 C. A. J. Hooper, L. Cardo, J. S. Craig, L. Melidis, A. Garai, R. T. Egan, V. Sadovnikova, F. Burkert, L. Male, N. J. Hodges, D. F. Browning, R. Rosas, F. Liu, F. V. Rocha, M. A. Lima, S. Liu, D. Bardelang and M. J. Hannon, *J. Am. Chem. Soc.*, 2020, **142**, 20651–20660.
42 J. T. Edward, *J. Chem. Educ.*, 1970, **47**, 261.
43 L. Avram and Y. Cohen, *Chem. Soc. Rev.*, 2015, **44**, 586–602.
44 Y. Cohen, L. Avram and L. Frish, *Angew. Chem., Int. Ed.*, 2005, **44**, 520–554.
45 J. Husson, J. Dehaudt and L. Guyard, *Nat. Protoc.*, 2013, **9**, 21–26.
46 J. T. Chantson, M. Vittoria Verga Falzacappa, S. Crovella and N. Metzler-Nolte, *ChemMedChem*, 2006, **1**, 1268–1274.
47 G. Dirscherl and B. König, *Eur. J. Org. Chem.*, 2008, 597–634.
48 S. Chakraborty and G. R. Newkome, *Chem. Soc. Rev.*, 2018, **47**, 3991–4016.
49 N. Zhang, J. Yang, R.-X. Hu and M.-B. Zhang, *Z. Anorg. Allg. Chem.*, 2013, **639**, 197–202.
50 H. Hofmeier and U. S. Schubert, *Chem. Soc. Rev.*, 2004, **33**, 373–399.
51 R. G. Pearson, *J. Am. Chem. Soc.*, 1963, **85**, 3533–3539.
52 A. Isidro-Llobet, M. Álvarez and F. Albericio, *Chem. Rev.*, 2009, **109**, 2455–2504.
53 L. Allouche, A. Marquis and J.-M. Lehn, *Chem. – Eur. J.*, 2006, **12**, 7520–7525.
54 P. W. Atkins and J. De Paula, *Physikalische Chemie. Hauptband*, Wiley-VCH Verlag GmbH & Co. KGaA, Weinheim, 5. Auflage, 2013.
55 H. B. Albada, A.-I. Chiriac, M. Wenzel, M. Penkova, J. E. Bandow, H.-G. Sahl and N. Metzler-Nolte, *Beilstein J. Org. Chem.*, 2012, **8**, 1753–1764.
56 H. B. Albada, P. Prochnow, S. Bobersky, S. Langklotz, J. E. Bandow and N. Metzler-Nolte, *ACS Comb. Sci.*, 2013, **15**, 585–592.